Imaging a CO_2 plume over the Sleipner CCS facility using FWI of sparse OBN data

Introduction

Carbon capture and storage (CCS) is one of the key technologies for reducing CO_2 emissions. A vital component of CCS is the monitoring of any facility to ensure storage integrity and track CO_2 plume movement. Imaging performs a crucial role however, acquiring seismic data over storage sites can be challenging due to the presence of co-located structures (platforms, production facilities, windfarms etc.) and the requirement for CCS monitoring to be cost effective. One solution is to utilise a short streamer acquisition (XHR) to provide a high-resolution dataset which can be combined with a sparse array of Ocean Bottom Nodes (OBN) which enable velocity model building via Full Waveform Inversion (FWI) (David et al., 2023). Achieving a high-resolution velocity model with FWI requires performing successive iterations using progressively higher frequency bands. At low frequencies, FWI mostly utilises diving wave energy where the sparsity of the nodes is not a problem. At higher frequencies more reflection energy is utilised, and the node data can be processed through to wavefield separation and up-down deconvolution (UDD) (Amundsen, 2001) to provide a reflectivity dataset for the FWI. A problem can arise here with sparse node acquisition due to inadequate sampling of the shallow subsurface and the higher frequency velocity updates are thereby compromised.

In this paper a study over the CCS Sleipner field is used to demonstrate how using the full wavefield including surface multiple energy can enhance the FWI imaging in the shallow subsurface, greatly improving the suitability of such sparse node acquisition for imaging over CCS sites. A data reconstruction method is used to produce a high-resolution image of the CO_2 plume and is compared to an FWI result produced from UDD reflectivity data.

Short streamer XHR and OBN acquisition over the Sleipner field

A sparse grid, 500 x 525 m of 47 OBNs were deployed using a cost-effective drop-down deployment and recovery operation. These are shown as the yellow dots on the survey plan in Figure 1. The nodes complemented the XHR system also shown in Figure 1 which acquired data at a 1 ms sample rate, with a maximum offset of 150 m and a record length of 3000 ms. The narrow streamer spread and dense shot grid provided a bin size of 1.56 m x 3.125 m. The node data were recorded simultaneously with the XHR data using the shots fired from the streamer vessel.

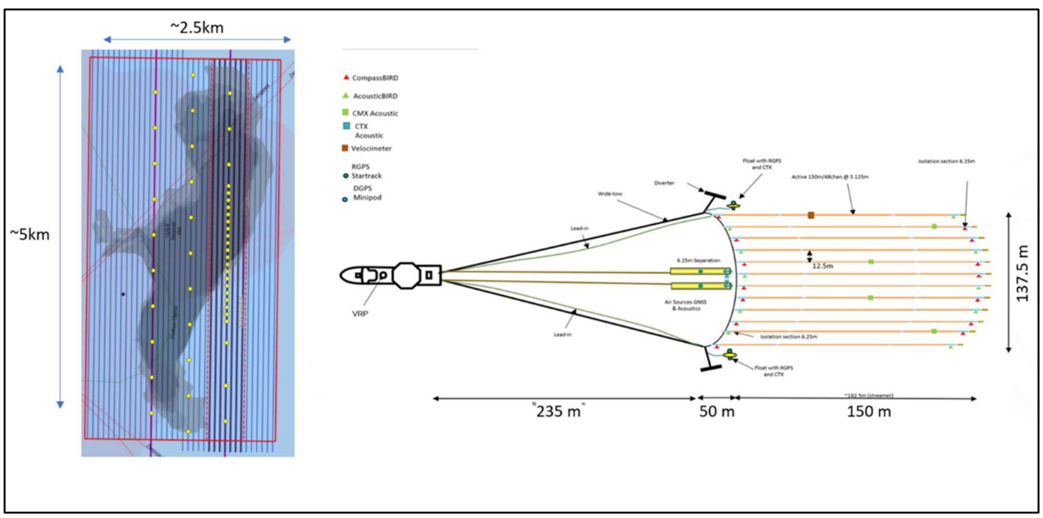

Figure 1 *Survey plan and boat diagram of the XHR and sparse ocean bottom node acquisition (node locations shown as yellow dots).*

Velocity model building using FWI

A dynamic matching FWI (DM FWI) (Mao et al. 2020) was first run up to 8 Hz utilising diving wave and near surface reflection energy.

Higher frequency updates were then performed at frequencies up to 12, 15, 25, 35, 45 and 60 Hz respectively. For these updates two routes were explored. Firstly, the node data utilising both the hydrophone and vertical geophone components were processed through to UDD. This provided a dataset with the surface reflection events (ghosts and surface multiples) removed. It should be noted that UDD assumes local homogeneity which breaks down in more complex geological regimes. For Sleipner however this assumption is generally valid. The higher frequency updates were performed on this dataset using the DM FWI method. An alternate FWI scheme was performed using the full wavefield, hydrophone (P) data. In this method the free surface reflectivity was included in the inversion and a data reconstruction FWI (Zuberi et al., 2023) was used. to mitigate the effects of guided waves. In the data reconstruction method, the acoustic equivalent data are reconstructed by matching the observed to the modelled (acoustic propagation) data. A filter is derived for each receiver gather which mitigates for the elastic effects of guided waves which cannot be explained by acoustic modelling.

Comparison of FWI results: UDD reflectivity vs Full Wavefield (P) data

Figure 2 shows the velocity models after the 25 Hz update from the two methods. Also shown are the FWI images produced from the derivatives of these models. The CO_2 plume can be seen as the notable slow velocity indicated by the red arrows. Both updates show good definition of the CO_2 plume however due to the limited illumination of the shallow subsurface provided by the sparse node UDD dataset the velocity model in the shallow section is less well defined compared to the full wavefield version. This difference is particularly apparent in the FWI images. It can also be seen in the UDD version that fast velocity bands are present in the model which are absent from the full wavefield version.

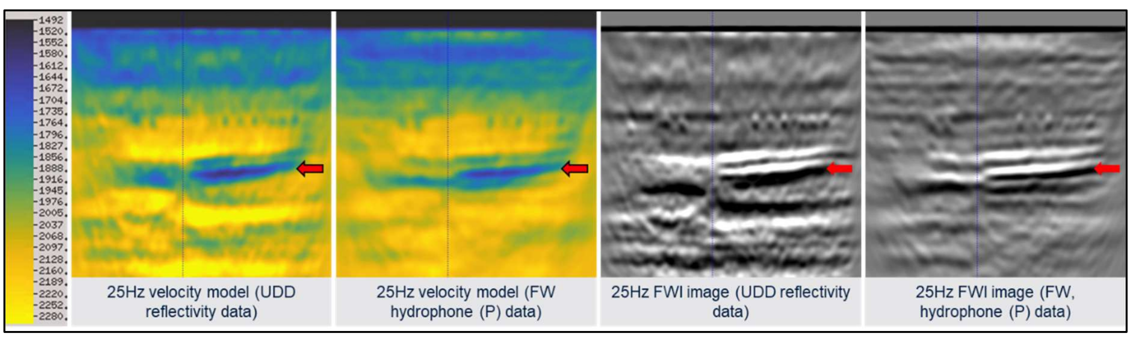

Figure 2 *Comparisons of the velocity models and FWI images for the 25 Hz updates produced using UDD reflectivity data vs the full wavefield (P) data. Red arrows indicate the location of the CO_2 plume.*

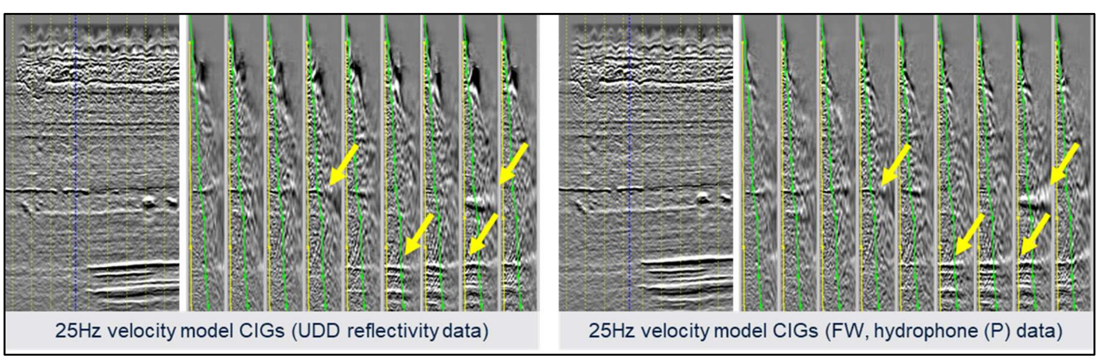

Figure 3 *Kirchhoff depth migration and common image gather comparisons: 25 Hz FWI velocity updates produced by using UDD reflectivity data vs the full wavefield (P) data.*

A further assessment of the two models was made by using them to produce Kirchhoff depth migrations of the UDD data and comparing the gather flatness of the common image gathers (CIGs). Figure 3 compares migrated images and CIGs for both cases. The arrows marked on the gathers indicate key events around the CO_2 plume and injectites where gather flatness is much improved in the full wavefield result compared to the UDD. The poor gather flatness in the UDD result corresponds to the fast velocity bands seen in the FWI (UDD reflectivity) velocity model in Figure 2. These fast velocity bands produce erroneous reflection events on the corresponding image also shown in Figure 2.

Higher frequency updates: 60Hz

FWI updates were performed on the full wavefield data until a 60 Hz velocity model was achieved. The 60 Hz velocity update along with the corresponding FWI image was then compared to a migrated UDD section. A further QC of the model was made by a comparison with the depth migrated XHR data, both fully processed and raw (including multiples). These comparisons are shown in Figure 4. The 60Hz FWI image compares well with both the UDD and XHR migrated sections. The obvious surface multiples in the raw XHR image are not evident in the FWI image. This suggests using the full wavefield produces reliable updates for these higher frequencies.

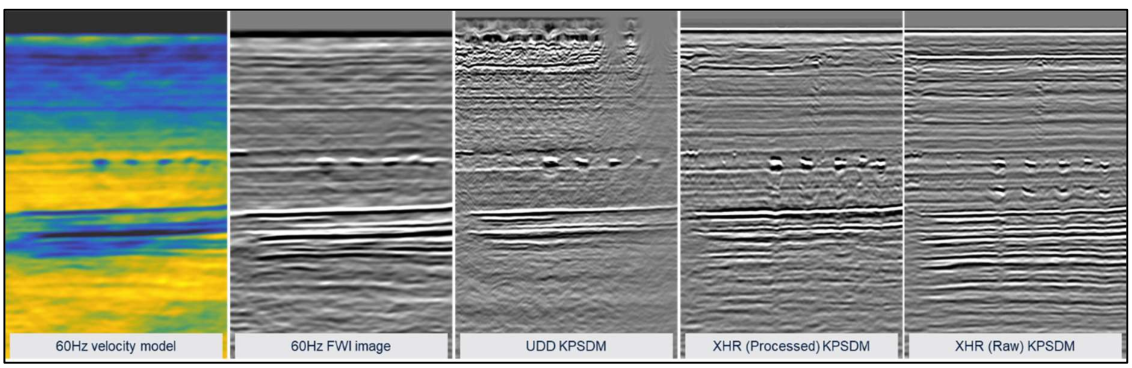

Figure 4 *Comparison of 60 Hz FWI velocity model with derived image, migrated UDD dataset, migrated XHR (processed) dataset and migrated XHR (Raw) dataset.*

FWI without free surface performed on primaries only data.

To further evaluate the impact of free surface multiples in the sparse node FWI imaging a ‘primaries only’ dataset was constructed via acoustic modelling of the 60 Hz velocity model. An FWI sequence was then performed on these data with no free surface reflectivity included in the forward modelling. Figure 5 contrasts the velocity updates at 8 Hz for the full wavefield and the primaries only data. The resulting velocity model from the primaries only data is characterised by anomalous high velocity regions in the shallow section with the imprint of the sparse node sampling evident. There are also regions of high and fast velocities above the plume and the resulting common image gathers show a poorer response in terms of flatness. This highlights the benefit of using the full wavefield with the multiple energy providing an increased illumination of the shallow subsurface which cannot be obtained using primaries alone.

Conclusions

Physical and cost constraints can place a limitation on seismic acquisition configurations over CCS storage sites. Ocean bottom nodes provide an important complement to short streamer XHR surveys providing a means to achieve a high-resolution velocity model. To make such acquisitions cost effective a sparse grid is desirable. Multiples are a vital component for velocity model building over such grids, and we demonstrate their utilisation by exploiting the full wavefield utilising a data reconstruction FWI methodology. This can make sparse node acquisition for CCS site imaging viable. Using the full wavefield avoids the requirement to process the node data through to up-down deconvolution. Furthermore, the velocity model created from a UDD reflectivity dataset suffers from poor illumination of the shallow subsurface which can produce inaccurate velocities at the CO_2 plume level. Using the full wavefield, incorporating multiple energy, can mitigate for this loss of illumination and provide a more accurate velocity model at the plume level. Avoiding the requirement to process the node data through to UDD may also reduce the cost and timescales of such CCS imaging projects.

A future study could be to combine the short offset XHR data with the node data in a joint-FWI. This has the potential for producing higher frequency images with increased resolution required for CO_2 monitoring. It is also acknowledged that here we have discussed only acoustic FWI and its associated limitations in explaining guided wave energy at the near surface. Elastic FWI modelling is suggested as a possibility for enhancing the imaging of the near surface over these types of CO_2 storage monitoring surveys.

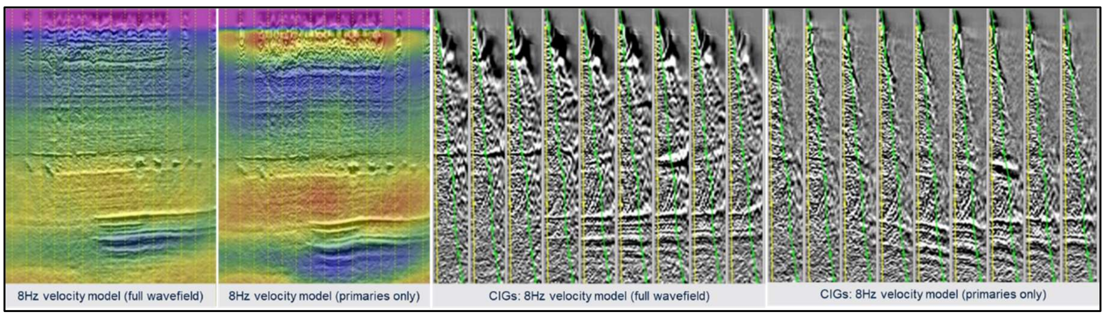

Figure 5 *8 Hz velocity model overlays on KPSDM imaged UDD data and common image gathers comparing results using the full wavefield input vs primaries only data.*

Acknowledgements

The authors thank Equinor Energy AS and CLIMIT program for their support and collaboration on the XHR/OBN Sleipner acquisition, the TGS imaging team in Woking, UK for their work on the FWI and XHR data processing and TGS New Energy Solutions for their permission to share the data.

References

David S., Zuberi M.A.H., Cho E., Baldock S., Stokes S., and Stock G. [2023]: Unlocking advanced imaging for CCS using cost effective acquisition solutions, *The Fourth EAGE Global Energy Transition Conference and Exhibition*, 2023.

Amundsen L. [2001]: Elimination of free-surface related multiples without need of a source wavelet, *Geophysics*, **66**, no.1, 327-341.

Mao J., Sheng J., Huang Y., Hao F. and Liu F. [2020]: Multi-Channel dynamic matching full-waveform inversion, *SEG 90th Annual Meeting*, 2020.

Zuberi M.A.H, Cho E., Seher T. and Myklebust R. [2023]: Mitigating the effects of guided waves in OBN data for acoustic FWI using data reconstruction: A data example from the Yggdrasil area, *IMAGE 2023 extended abstract*.